This is a repository copy of *Improved near surface wind speed predictions using Gaussian process regression combined with numerical weather predictions and observed meteorological data*.

White Rose Research Online URL for this paper:
http://eprints.whiterose.ac.uk/129379/

Version: Accepted Version

1 Improved near surface wind speed predictions using Gaussian process regression combined with numerical weather
2 predictions and observed meteorological data.

3 Authors: Victoria Hoolohan[a, b], Alison S. Tomlin[b], Timothy Cockerill[c]
4
5 [a] Doctoral Training Centre in Low Carbon Technologies, University of Leeds, Leeds LS2 9JT, UK
6 [b] School of Chemical and Process Engineering, University of Leeds, Leeds LS2 9JT, UK
7 [c] Centre for Integrated Energy Research (CIER), Leeds LS2 9JT, UK
8

9 ABSTRACT

10 This study presents a hybrid numerical weather prediction model (NWP) and a Gaussian process regression (GPR) model
11 for near surface wind speed prediction up to 72 hours ahead using data partitioned on atmospheric stability class to
12 improve model performance. NWP wind speed data from the UK meteorological office was corrected using a GPR
13 model, where the data was subdivided using the atmospheric stability class calculated using the Pasquill-Gifford-Turner
14 method based on observations at the time of prediction. The method was validated using data from 15 UK MIDAS (Met
15 office Integrated Data Archive System) sites with a 9 month training and 3 month test period. Results are also shown for
16 hub height wind speed prediction at one turbine. Additionally, power output is predicted for this turbine by translating
17 hub height wind speed to power using a turbine power curve. While various forecasting methods exist, limited methods
18 consider the impact of atmospheric stability on prediction accuracy. Therefore the method presented in this study gives a
19 new way to improve wind speed predictions. Outputs show the GPR model improves forecast accuracy over the original
20 NWP data, and consideration of atmospheric stability further reduces prediction errors. Comparing predicted power
21 output to measured output reveals power predictions are also enhanced, demonstrating the potential of this novel wind
22 speed prediction technique.

1. INTRODUCTION

26 An increasing awareness of the environmental impacts of anthropogenic greenhouse gas emissions has motivated a
27 dramatic increase in renewable energy, a significant proportion of which is produced by wind turbines. As of October
28 2016 there is over 14 GW of installed wind capacity in the UK [1], although this is set to rise further as the UK
29 government continues towards the target of 15% renewable energy by 2020. While the wind resource in the UK is
30 abundant, its variable and intermittent nature can cause issues with maintaining a secure and constant supply of
31 electricity. Wind power predictions allow supply and demand of electricity to be carefully managed, reducing the cost
32 impact on power system operators and aiding the integration of wind energy in the electricity system [2]. However, their
33 accuracy has a direct impact on grid reliability and profitability. Barthelmie et al. [3] show that short term forecasting can
34 increase the price obtained for electricity sold by around 14% but that the value was dependent on the forecast accuracy.

35 Wind power is highly sensitive to terrain, local and regional weather systems and obstacles such as buildings. Wind
36 exhibits seasonal and diurnal patterns alongside stochastic high frequency variability [4]. Consequently, it is complex to

accurately predict in advance. Forecasting wind power output intrinsically relies on estimates of wind speed. Whilst methods for predicting wind power exist, improvements in accuracy could still be made. Current methods cover various time scales, from less than a minute to days or weeks in advance. Reviews of currently available techniques are given by [5] and [6]. Methods can be broadly categorised as statistical, numerical weather prediction (NWP) or hybrid models.

Statistical methods predict wind speed by analysing patterns in observed time series. Examples include a seasonally adjusted ARMA (auto-regressive moving average) model presented by Torres et al. [7] which is used to predict wind speeds up to 10 hours in advance. The study showed improvements over a persistence model but noted that the model was only valid over short time periods. Other examples of statistical methods include an f-ARIMA (fractional auto-regressive integrated moving average) model presented by Kavasseri and Seetharaman [8]. In this model, results are shown to be superior to a persistence model up to 48 hours. Statistical prediction methods can be effective over short time scales (up to a few hours) but cannot usually predict accurately further in advance.

NWP models aim to resolve complex numerical systems to establish global and local weather patterns based on observed initial conditions. While these are more accurate than statistical models over longer time periods, some difficulty is encountered in solving numerical systems at a high resolution due to the complexity of atmospheric conditions and high computational costs. NWP models are expensive to run and usually only available from large organisations such as government meteorological departments. A high quality NWP is provided by the UK meteorological office (the Met Office), which employs a 1.5 km resolution model across the UK nested within a lower resolution global model [9]. Other NWP models exist, such as MM5, Prediktor and HIRLAM [5]. NWP models can resolve complex systems of equations defining global and local weather systems. However, they can be limited by their horizontal resolution. At some sites, complex terrain can affect wind conditions within the 1.5 km in which they are resolved. Furthermore, different site characteristics can affect how predictions are adjusted to hub height wind speed predictions.

Hybrid systems combine a number of models, such as statistical and physical models. Of particular interest is the combination of NWP and statistical methods which allows reduced prediction errors compared to an NWP or statistical model used in isolation. For example, Larson and Westrick [10] use an NWP model in conjunction with statistical models such as artificial neural networks (ANN), support vector machines or conditional neural networks to predict wind speeds up to 2 hours ahead. The study looks at the use of off-site weather prediction data and shows an improvement over persistence forecasting. More recently, Wang et al. [11] presented an ANN model incorporating wavelet transform, variational mode decomposition and phase space reconstruction. Hybrid models incorporating GPR have not been extensively applied for wind speed prediction but there are a small number of previous studies. Zhang et al. [12] combine an autoregressive model with GPR for probabilistic wind speed forecasting. The model was used to predict mean hourly wind speed one hour ahead for wind speeds at 3 wind farms in China. Furthermore, Hu et al. [13] combine empirical wavelet transform, partial auto correlation function and GPR to predict wind speeds at one wind warm in China. The results are shown for both half hourly wind speed prediction (up to 2 hours ahead) and hourly wind speed prediction (up to 4 hours ahead). The model presented in this paper focuses on wind speed forecasts further in advance, presenting a hybrid NWP and GPR model for wind speed predictions up to 72 hours ahead and shows the impact of subdividing input data by atmospheric stability class. This study thus presents a novel contribution to the literature on GPR methods for wind speed forecasting.

Table 1 provides a summary of some of the currently available forecasting methods, and the results of applying these methods. The methods listed cover both wind speed and power forecasting methods and both hybrid and statistical forecasting techniques. The error metrics used to present results vary across the literature but an attempt is made to consolidate the results in a comparable way. For wind speed forecasting methods root mean squared error (RMSE), mean absolute error (MAE) and mean absolute percentage error (MAPE) are shown where possible. For wind power forecasting RMSE and MAE are normalised by capacity to allow comparison between installations of different sizes, giving NRMSE, NMAE and MAPE as comparison statistics for power forecasts. Definitions for RMSE, MAE and MAPE are given within the methodology section in equations 9, 10 and 11 whilst NRMSE and NMAE are defined in equations 13 and 14, all of which are given in section 3. Where sufficient detail is given in the literature, the results are shown in comparison to the persistence model. The persistence model forecasts wind speed or power by assuming the forecasted value is equal to that of the prior time period. It relies upon the auto correlation seen in wind speed and power time series and is commonly used as a benchmark for model performance to allow a comparison between forecasts when different datasets are used.

The wind speed prediction methods reviewed in Table 1 comprise of 4 statistical methods and 6 hybrid methods and cover a variety of timescales, from 1 hour ahead to 120 hours ahead. Firstly comparing short term predictions, Chen et al. [14], Wang et al. [11], Cadenas et al. [15], Hu et al.[13], Zhang et al. [12] and Torres at al [7] all present results for prediction up to 4 hours in advance. The method presented by Torres et al. [7] is a statistical method, whilst the other are hybrid methods. For these methods MAE varies between 0.18 and 1.14 ms^{-1} for a forecast 1 hour ahead and RMSE varies between 0.26 and 1.5 ms^{-1} for a forecast 1 hour ahead. For all these prediction methods except that presented by Wang et al. [11] the difference between MAE and RMSE for the different models is small. However, Wang et al. [11] show much lower errors. MAPE has a large variation for forecasts 1 hour ahead with the largest (21%) reported by Zhang et al. [12] and the smallest (8.5%) reported by Wang et al. [11]. The statistical model presented by Torres et al. [7] shows very similar results to the hybrid models presented by other authors at this timescale.

Kavasseri and Seetharaman [8], Torres et al. [7], Chen et al. [14] and Louka et al. [16] show results for forecasting methods further in advance, (5-120 hours ahead). The methods discussed by Kavasseri and Seetharaman [8] and Torres et al. [7] are statistical, whilst Chen et al. [14] and Louka et al. [16] present hybrid methods. The results from Kavasseri and Seetharaman are difficult to compare to the other methods due to how the results are aggregated. Of the other methods, Torres et al. [7] only show results for forecasts up to 10 hours ahead whilst Louka et al. [16] presents results up to 120 hours ahead and Chen et al. [14] up to 72 hours ahead. The hybrid methods presented by Louka et al. [16] and Chen et al. [14] perform much better than the statistical method presented by Torres et al. The hybrid method by Louka et al. [16] has an MAE of 2.04 ms^{-1} and an RMSE of 2.88 ms^{-1} as far ahead as 120 hours in advance, whilst the statistical method has an MAE of 2.5 ms^{-1} and an RMSE of 3 ms^{-1} at just 10 hours ahead. MAPE is only given by Chen et al. [14] hence this is not comparable. This indicates, as other literature suggests, that hybrid methods can perform well in the short term and frequently outperform statistical methods further in advance.

Five wind power prediction methods are compared in Table 1, including 3 hybrid methods and 2 statistical methods. The first statistical method, presented by Catalão et al. [17], is difficult to compare to the other techniques due to the errors shown. The only other statistical method is that presented by Ramirez-Rosado et al. [18] which reports results for forecasts up to 72 hours in advance. However, RMSE averaged over 3 time periods is shown (12-24 hrs ahead, 24-48 hrs

112 ahead and 48-72 hrs ahead), again making it difficult to compare to other methods. For the remaining three hybrid

113 methods only NMAE and NRMSE are compared as MAPE is only given in one case. The hybrid methods presented by

114 Chen et al. [19] and Shu et al. [20] report very similar results. The model presented by Chen et al. [19] reports results for

115 forecasts from 1 – 24 hours ahead, with an NMAE of between 7.5 and 11.1% and an NRMSE of between 11 and 16%.

116 The model given by Shu et al. [20] gives results for forecasts from 1 – 48 hours ahead, with an NMAE of between 7 and

117 15% and an NRMSE of between 11 and 21%. The model presented by Louka et al. [16] shows results for forecasts

118 between 24 and 120 hours ahead. This model seems to outperform others with an NMAE of between 11 and 15.5% and

119 an NRMSE of between 15 and 21%.

120 Whilst some comparisons are drawn between the methods presented in literature, it is important to note that the results

121 presented for these different methods use different datasets. Because of this direct comparisons are difficult. However, it

122 is still important to consider the range of errors reported by authors in other literature. This allows a consideration of the

123 range of errors which would be expected for a good forecast at different forecast horizons. In addition to this, in Table 1

124 the results presented by different authors are listed in comparison to the persistence forecast where this is possible. This

125 allows the improvement over a common benchmark model to be considered.

126

Table 1: Examples of the currently available forecasting techniques

Authors	Year	Speed or power	Method type	Method summary	Data	Forecast period	Results
Cadenas et al. [15]	2016	Speed	Hybrid	Nonlinear autoregressive exogenous model (NARX).	Wind speed data from La Mata, Mexico	1 hour ahead	MAE: 0.86 ms^{-1} (Persistence: 0.91^{-1}) MSE: 1.38 ms^{-1} (Persistence: 1.55 ms^{-1}) MAPE: 1.44% (Persistence: 11.96%)
Catalão, et al. [17]	2011	Power	Statistical	ANN + wavelet transform	All wind farms in Portugal that connect with the national electric grid.	3hours ahead.	MAE not given RMSE: 392.3 MW (Persistence not given) MAPE: 7% (Persistence 19%). Total capacity forecasted not given so cannot compare NRMSE.
Chen, et al. [14]	2013	Speed	Hybrid	Wavelet and Gaussian process	Wind farm in southern China. 15 turbines, installed capacity 2000kW	1-4 hours ahead and 1-3 days ahead daily mean wind speed	MAE: 0.72-1.6 ms^{-1} (Persistence: 0.74 – 1.83ms^{-1}) RMSE: 0.96 -2.04 ms^{-1} (Persistence: 1.0 – 2.23 ms^{-1}) MAPE: 11.24 -44% (Persistence: 11.1 – 42%)
Chen, et al. [19]	2014	Power	Hybrid	Gaussian process and NWP	3 wind farms in China. 3 years for 2 wind farms and 2.5 months for one.	1-24 hours. Results not shown separately	Results given for 4 wind farms: NMAE: 7.5-11.1% (Persistence 9.8 – 18.6%) NRMSE: 11.69 – 15.96% (Persistence 15.7 – 26.3%) MAPE: 7.6 – 11.12% (Persistence 10.1 – 18.4%) Best results for the largest wind farm.
Hu et al. [13]	2015	Speed	Hybrid	Empirical wavelet transform, partial autocorrelation function and GPR.	Wind speeds for 1 wind farm in China.	Up to 2 hours ahead for a half hourly model and 4 hours ahead for an hourly model.	Hourly model: MAE: 1.13 – 1.43 ms^{-1} (Persistence: 1.35 – 1.65 ms^{-1}) RMSE: 1.22 – 1.6 ms^{-1} (Persistence: 1.45 – 1.88 ms^{-1}) MAPE: 1.18-18.39% (Persistence: 12.84 – 21.76%)
Kavasseri and Seetharaman [8]	2009	Speed	Statistical	f-ARIMA	Wind speed from 4 potential wind farm sites in North Dakota	24 and 48 hours ahead	MAE not given RMSE: 5.35% (Persistence: 8.43%) MAPE (24hrs): 33.18% (Persistence 45.2%).
Louka, et al. [16]	2008	Speed and Power	Hybrid	Kalman filtering to post process NWP	1 year wind speed and power data at Rokas wind farm	24, 48, 72, 96 and 120 hours ahead	Speed: MAE: 1.75 - 2.04 ms^{-1} RMSE: 2.38 – 2.88 ms^{-1} Power: NMAE: 11 - 15.5%;

							NRMSE: 15 - 20.5% MAPE not given, comparison to persistence not given.
Ramirez-Rosado, et al. [18]	2009	Power	Statistical	Two ANN methods (FORECAS and SGP)	Wind farm with rated power of 21,600kW, 12 turbines of 1.8MW.	0.5 - 72 hours, time step 0.5 hours.	Average RMSE given 3 time periods: 12-24h, 24-48h and 48-72h. FORECAS: 14-19.7%, SGP: 14-18.8%, Persistence: 31.2- 37.5%. MAE and MAPE not given
Shu et al. [20]	2009	Power	Hybrid	Two stage hybrid network with Bayesian clustering and SVR.	74 MW wind farm in Oklahoma, US.	1-48 hours ahead	Errors given for 1, 24 and 48hrs. NMAE: 7-15% (Persistence 8-25%), NRMSE: 11-21% (Persistence 11-34%) MAPE not given
Torres, et al. [7]	2005	Speed	Statistical	ARMA	5 locations, 9 years. Wind measured every 10 mins at 10m and averaged over 1 hour.	up to 10 hours ahead	MAE: 0.9 - 2.5 ms^{-1} (Persistence 0.9 - 2.9 ms^{-1}) RMSE: 1.2 - 3 ms^{-1} (Persistence 1.25 - 3.7 ms^{-1}). MAPE not given
Wang et al. [11]	2017	Speed	Hybrid	Hybrid wavelet neural network optimised by genetic algorithm	Hourly wind speed for spring and autumn at one site in China	1,2,4,6 hours ahead	MAE: 0.187-0.269 ms^{-1} (Persistence 0.74-1.38 ms^{-1}) RMSE: 0.235-0.34 ms^{-1} (Persistence 0.95-1.72 ms^{-1}) MAPE: 8.44 – 12.02% (Persistence 31.4 – 58.5%)
Zhang et al. [12]	2016	Speed	Hybrid	Hybrid auto regressive and GPR model	Mean hourly wind speed at 3 wind farms in China	1 hour ahead	MAE: 0.79 – 0.87 ms^{-1} (Persistence 0.85 – 1.1 ms^{-1}) RMSE: 1.05- 1.13 ms^{-1} (Persistence 1.12 – 1.52 ms^{-1}). MAPE: 10.03 – 21.1% (Persistence 10.44 – 19.97%)

129

130   The results shown indicate that hybrid methods can outperform statistical methods, particularly for longer term forecast

131   periods. The combination of NWP models and statistical methods results in better predictions. Hence this paper develops

132   a hybrid NWP and Gaussian process regression (GPR) model to predict near surface wind speeds up to 72 hours ahead. It

133   also considers whether including information on stability conditions can aid model performance. In summary, a three

134   hourly wind speed forecast from an NWP is corrected using a GPR model. The simple GPR model results are compared

135   to a model where the data is divided using the atmospheric stability class calculated from observations at the time of

136   prediction. The key innovation in this paper is the use of atmospheric stability class to partition data in the hybrid NWP

137   and GPR model. Atmospheric stability is a measure of the atmosphere's tendency to encourage or reduce vertical motion

138   [21]. Under stable conditions, vertical motion is suppressed and under unstable conditions, vertical motion is encouraged.

139   Both stable and unstable conditions are usually associated with low mean wind speeds. In the absence of heat flux at the

140   surface, the atmosphere is said to be neutral, with neutral conditions usually associated with higher mean wind speeds.

141   Atmospheric stability is an important component in modelling wind characteristics as it can affect atmospheric

142   circulation and momentum transfer [22]. Because of this, it is interesting to investigate the impact of atmospheric

143   stability on NWP accuracy of wind speed forecasts and whether partitioning data can improve forecast accuracy.

144   In this paper, the model is introduced, and the results are shown for a selection of 15 weather observation sites across the

145   UK. The model is also tested for the prediction of hub height wind speeds for one turbine in the UK. At this site,

146   predicted wind speeds are compared to measured wind speed. Finally, the impact of improved wind speed forecast on

147   power forecasting is considered. Section 2.1 introduces the GPR model, giving an overview of the mathematical

148   concepts. Section 2.3 gives the definition of atmospheric stability used in the current work, its potential role in wind

149   forecasting, and methods for calculation. Sections 2.2 and 2.4 give details of the model formulation and data used to test

150   the model, section 3 presents the results and section 4 gives conclusions and outlines the potential for further work.

2. METHODOLOGY
2.1 Gaussian process regression

153   GPR is a supervised learning method where an input-output mapping is learnt from empirical data [23]. It is a regression

154   technique which does not initially restrict the relationship between the target and input variables to a specific form. It is a

155   non-parametric Bayesian modelling technique, allowing a flexible model. Prior knowledge is combined with observed

156   data to determine posterior predictive distributions for further test inputs.

157   GPR has been used for prediction in a number of applications, for example spectroscopic calibration [24], robot control

158   [25] and image processing [26]. Through these applications, GPR has shown an ability to predict well in situations where

159   complex nonlinear relationships exist between variables. Because of this, it could prove to be a good method for wind

160   speed prediction, given the typically complex patterns and relationships between wind and other weather variables. Chen

161   et al. [19] describe a method in which an NWP model is combined with a GPR model to predict wind speeds up to 1 day

162   ahead. The corrected wind speeds are used to predict wind power using another GPR model. In this example, three data

163   sets from different wind farms in China are used to validate the method, reporting reductions in mean absolute error

164   compared to an Artificial Neural Network (ANN) model. In a different study Chen et al. [14] present the potential for a

165   composite wavelet analysis and GPR forecasting technique. Small improvements over a simple GPR model were noted,

166   demonstrating that the concept merits further investigation.

167 GPR aims to identify a relationship between input variables and target variables, based on the observational data

168 available. The aim is to create a function that satisfies $y_i = f(x_i) + \varepsilon_i$ where y is the target variable, x are the input

169 variables and ε is normally distributed additive noise. Rasmussen and Williams [23] provide an extensive mathematical

170 background of GPR, of which a summary is provided here. The Gaussian process $f(\mathbf{x})$ is completely specified by its

171 mean and covariance function, $f(\mathbf{x}) \sim GP(m(\mathbf{x}), k(\mathbf{x}, \mathbf{x}'))$, where the mean and covariance functions are given by

172 equations (1) and (2).

$$m(\mathbf{x}) = E[f(\mathbf{x})] \tag{1}$$

$$k(\mathbf{x}, \mathbf{x}') = E[(f(\mathbf{x}) - m(\mathbf{x}))(f(\mathbf{x}') - m(\mathbf{x}'))] \tag{2}$$

173 This is used to define a distribution over functions which can be updated using training data. The prior distribution is the

174 initial specification of the distribution which gives information on the mean and covariance functions used. Given a

175 training set $D = (\mathbf{X}, \mathbf{y})$ the target is to predict the function values f_* given inputs $\mathbf{X}_*$. Being a linear combination of

176 Gaussian variables, $\mathbf{y}$ is also Gaussian, with distribution $\mathbf{y} \sim N(m(\mathbf{x}), K(\mathbf{X}, \mathbf{X}) + \sigma^2 \mathbf{I}$ where $K_{i,j} = k(\mathbf{x_i}, \mathbf{x_j})$. The joint

177 distribution of the training data and the predicted output is given by equation (3) [27].

$$\begin{bmatrix} \mathbf{y} \\ \mathbf{f}_* \end{bmatrix} \sim N \left(\begin{matrix} m(\mathbf{X}) \\ m(\mathbf{X}_*)' \end{matrix} \begin{bmatrix} K(\mathbf{X}, \mathbf{X}) + \sigma^2 \mathbf{I} & K(\mathbf{X}, \mathbf{X}_*) \\ K(\mathbf{X}_*, \mathbf{X}) & K(\mathbf{X}_*, \mathbf{X}_*) \end{bmatrix} \right) \tag{3}$$

178 The principle of joint Gaussian distributions allows the prediction results for the target to be inferred from the mean

179 function $\bar{\mathbf{f}}_*$ and the covariance function $cov(\mathbf{f}_*)$ given by equations (4) and (5).

$$\bar{\mathbf{f}}_* = m(\mathbf{X}_*) + K(\mathbf{X}_*, \mathbf{X})[K(\mathbf{X}, \mathbf{X}) + \sigma^2 \mathbf{I}]^{-1}(\mathbf{y} - m(\mathbf{X})) \tag{4}$$

$$cov(\mathbf{f_x}) = K(\mathbf{X}_*, \mathbf{X}_*) - K(\mathbf{X}_*, \mathbf{X})[K(\mathbf{X}, \mathbf{X}) + \sigma^2 \mathbf{I}]^{-1} K(\mathbf{X}, \mathbf{X}_*) + \sigma^2 \mathbf{I} \tag{5}$$

180 The covariance is a crucial part of the model specification, as it includes assumption about the functional relationship.

181 Despite this establishing the correct covariance function for a regression problem is a significant issue in the inference

182 process. The squared exponential (SE) covariance function is a commonly used covariance function due to its ease of

183 interpretation and flexibility [28] and hence is used in this work. The squared exponential covariance function is given by

184 equation (6),

$$cov_{SE}(\mathbf{X}, \mathbf{X}') = \sigma^2 exp\left(-\frac{(\mathbf{X} - \mathbf{X}')^2}{2l^2}\right) \tag{6}$$

185 where σ^2, l are the signal variance and length scale respectively. In order to maximise the flexibility of the model,

186 parametric covariance functions are used and the hyperparameters are inferred from observed data. The process of

187 learning the hyperparameters, $\theta = (l, \sigma^2)^T$, from data is achieved by maximising the log likelihood function [19], given

188 by equation (7).

$$\ln P(\mathbf{y}|\theta) = \frac{1}{2} ln|\mathbf{K}| - \frac{1}{2} \mathbf{y}^T \mathbf{K^{-1}} \mathbf{y} - \frac{n}{2} \ln(2\pi) \tag{7}$$

189

190 For a multidimensional input variable a separate length scale is calculated for each model variable, and the relative

191 importance of different inputs can be inferred from the observed data, a process which is known as automatic relevance

192 determination (ARD).

2.2 Data

The predicted wind speeds which are used to inform the hybrid model are taken from an NWP model developed by the Met Office. This NWP model provides three hourly forecasts up to 5 days in advance, employing a global forecast model to predict longer range weather forecasts (48+ hours ahead) combined with a mesoscale model to generate a more accurate short range forecast. The forecast data used in this work are a weighted combination of the Met office UKV and Euro4 models. UKV is a variable resolution deterministic model, with a resolution of 1.5 km over the UK and decreased resolution at the model boundaries to aid integration in a nested model. Euro4 is a 4 km resolution deterministic model covering Europe. UKV runs up to 36 hours in advance and Euro4 up to 120 hours. The forecast data is available from the UK governmental public data website [29] for over 6000 sites. The meteorological observations which have been used for reference have been taken from the Met Office Integrated Data Archive System (MIDAS), available from the British Atmospheric Data Centre (BADC) [30]. The archive consists of UK land surface observations, global marine observations, and a selection of radiosonde observations both in the UK and at international stations operated by the Met Office. This data provides hourly observations of a selection of meteorological variables including wind speed and direction, cloud cover, temperature, air pressure and humidity amongst others. The MIDAS stations are set up so that the observation data can be the best quality possible with details given by the BADC [30]. Cup anemometers are used to measure wind speed, at a height of 10 m above ground level. The site must be free from obstructions to avoid measurements in the wake of obstructions and quality control is performed to avoid inclusion of spurious data where possible. For example, automatic algorithms are applied to ensure consistency of wind measurements with other local stations. Not all weather variables are available at every MIDAS site and data coverage is variable, dependent on factors such as equipment failure. Because of this, 15 sites were chosen across the UK where sufficient data was available for analysis. The MIDAS datasets are taken from various locations across the UK, with different weather conditions and site characteristics across the selection. The sites were categorised into 4 types; rural, urban, mountain and coastal. Categories were chosen for the sites based on visual inspection of the site itself and the local area, considering the proximity to coastline, building density, elevation and terrain complexity. The model performance was considered within the different categories as well as overall. The locations and classification of these sites are shown in Figure 1.

To demonstrate the potential for wind power prediction, the model was also tested for one location in the UK where hub height wind speed and power was available. The data comprised of measured wind speed data at approximately 65 m above ground level and power output from a 1.5 MW turbine in a suburban location.

Figure 1: Map of 15 MIDAS locations across the UK, including site classification

221

2.3 Treatment of Atmospheric Stability

223 Atmospheric stability is a measure of the atmosphere's tendency to encourage or deter vertical motion [21]. Neutral
224 conditions occur during high winds and when cloud cover prevents strong heating or cooling of the earth's surface.
225 Unstable conditions occur when strong surface heating and low wind speed conditions occur, encouraging vertical
226 motion of air. Stable conditions usually occur as a result of a cool surface, either the earth at night or over cool oceans.
227 The flow of air is affected by atmospheric stability and consequently a number of different aspects of wind power
228 forecasting can be affected. For example, Peterson et al. [31] document the difference in vertical wind profiles under
229 different stability conditions. The difference in the power law under different stability conditions is also explored by
230 Irwin [32]. This was further investigated empirically by Focken and Heinemann [33], using data from a meteorological
231 observation mast at Cabouw in the Netherlands.

232 Numerous methods exist for classifying stability, each requiring a range of meteorological parameters for calculation.
233 Some examples include the Obukhov length, Richardson number, temperature gradient, wind speed ratio and Pasquill-
234 Gifford stability class. The main issue surrounding calculation of some stability parameters is that they require estimates
235 of variables such as frictional velocity and heat flux which are not commonly available from either forecasts or
236 meteorological observations. The Pasquill-Gifford method was developed to categorise the stability class based upon
237 variables that are commonly measured at meteorological stations. The method uses solar insolation as an indication of
238 convective turbulence and wind speed as an indication of mechanical turbulence [21]. This method for calculating
239 stability was developed predominantly for the purpose of pollutant dispersion models, however has become a commonly
240 used classification scheme. It requires wind speed at one height, daytime solar insolation or night time cloud cover. This
241 was further modified by Turner by using net radiation index (NRI) to estimate solar insolation based on cloud cover and

cloud ceiling height, resulting in the Pasquill-Gifford-Turner (PGT) method for stability condition classification. The PGT method classifies 7 different stability conditions as given in Table 2.

Table 2: Stability categories for PG and PGT stability methods

PGT class	Stability condition
1	Highly unstable or convective
2	Moderately unstable
3	Slightly unstable
4	Neutral
5	slightly stable
6	Stable
7	Extremely stable

The first step in obtaining the stability classification is to calculate the insolation class number. This is obtained based on solar altitude as outlined in Table 3. NRI is calculated using the algorithm given in Figure 2, where cloud cover is given in tenths, with 1/10 indicating low cloud cover and 10/10 indicating opaque cloud. Finally, using NRI and wind speed, the stability classification is obtained from Table 4.
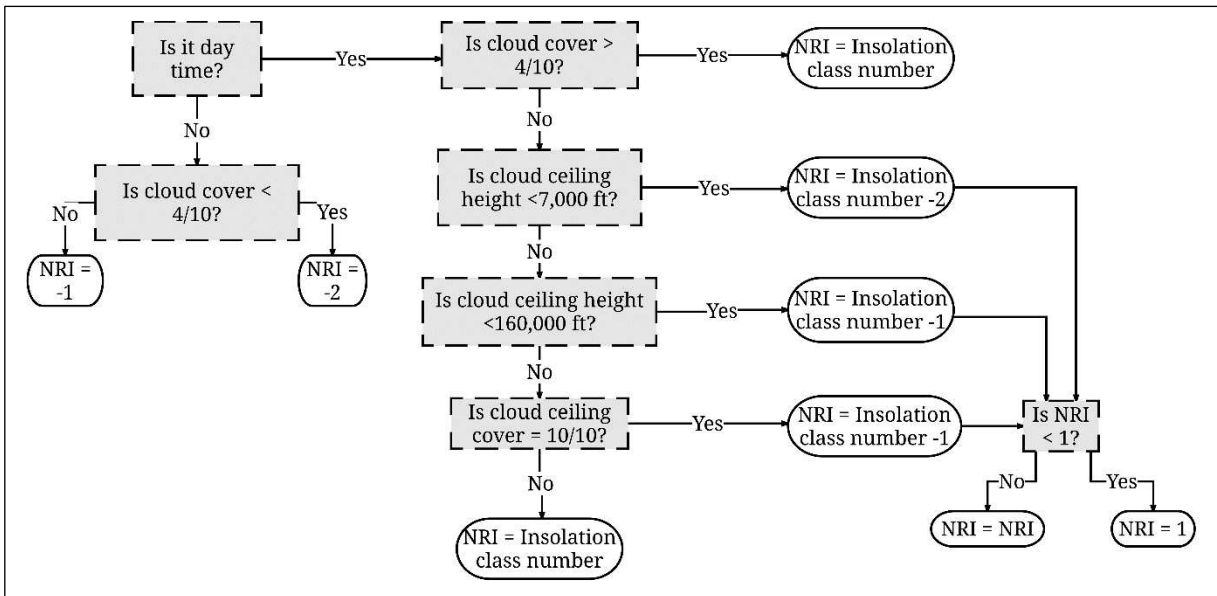
Table 3: Insolation class number

Solar Altitude (φ)	Insolation	Insolation class number
$60 < \varphi$	Strong	4
$35 < \varphi \leq 60$	Moderate	3
$15 < \varphi \leq 35$	Slight	2
$\varphi \leq 15$	Weak	1

Figure 2: Algorithm for calculating net radiation index [34]

Table 4: PGT stability classes

Wind speed (ms^{-1})	Net radiation index (NRI)						
	4	3	2	1	0	-1	-2
0-0.7	1	1	2	3	4	6	7
0.8-1.8	1	2	2	3	4	6	7
1.9-2.8	1	2	3	4	4	5	6
2.9-3.3	2	2	3	4	4	5	6
3.4-3.8	2	2	3	4	4	4	5
3.9-4.8	2	3	3	4	4	4	5
4.9-5.4	3	3	4	4	4	4	5
5.5-5.9	3	3	4	4	4	4	4
≥6	3	4	4	4	4	4	4

254   The PGT method allowed stability conditions to be estimated based on MIDAS observations. However, the forecasted

255   variables available from the Met office forecast data do not include sufficient details of cloud conditions to allow the use

256   of the PGT method. Because of this stability conditions used in this work have been based on MIDAS observations at the

257   time of the prediction. In future, if further forecasted variables were available, the work could be extended to explore the

258   impacts of using predicted stability conditions.

259   ## 2.4 Model Set-up

260   An introduction to the method is given above, however, the model inputs and outputs require further definition. Due to

261   the variables required to estimate stability conditions, only sites where information on wind, cloud depth and coverage

262   was available were considered. From the MIDAS sites across the UK with sufficient data, 15 sites were investigated. The

263   location of these sites was shown in Figure 1. Further to this, for one turbine in the UK hub height wind speed and power

264   output data was available. Results are shown for the prediction of hub height wind speed at this site.

265   As detailed in section 2.1 the model develops a relationship between target variable **y** and input variables **x** of the form

266    $y_i = f(\mathbf{x}_i) + \varepsilon_i$. The model is a multivariate regression model with 4 predictor variables, the Met Office forecast and 3

267   hours of observed data prior to the beginning of the forecast. Forecasts up to 72 hours in advance were considered, at 3

268   hour intervals. Hence the predictor variables are given by equation (8).

$$\mathbf{X}_t = [\mathbf{m}_t, \mathbf{y}_{t-h-1}, \mathbf{y}_{t-h-2}, \mathbf{y}_{t-h-3}] \text{ for } t = 4, \dots, n \tag{8}$$

269   Where:

$t =$	time of observation
$\mathbf{m}_t =$	Met Office forecast at time (ms^{-1})
$\mathbf{y}_t =$	observed wind speed at time t (ms^{-1})
$h =$	hour of forecast

270   Section 3.1 presents the results of the forecast model for predicting wind speed at 10 m above ground level for 15

271   MIDAS sites across the UK. In this case, the target variables, **y**, are the MIDAS observations at the site. Section 3.2

272   presents results of the forecast model for wind speed prediction at hub height for a suburban location in the UK. Finally,

273   section 3.3 explores the potential impact of improved hub height wind speed forecasting on wind power forecasting. To

274   ensure an independent forecast, the data was split into a training dataset and a test dataset. The training dataset was used

275   to train model hyperparameters and the test dataset to assess the model performance. The training data are defined as the

276   concurrent observations and Met Office forecast data for the first 9 months of 2014 and the test data are same data from

277 the final 3 months of 2014. The observation data was available at hourly intervals and the forecast data at 3 hourly

278 intervals. This describes the formulation of the GPR model with no stability data. To test the impact of using atmospheric

279 stability to improve the model, the data was split into 7 stability classes and the model trained separately for each class.

280 From the variables available in the Met Office forecast an indication of forecasted stability conditions is difficult to

281 obtain, therefore currently this study uses the stability conditions at the time of the observation, as calculated from the

282 MIDAS data. Whilst in the case of an actual forecast scenario this information would not be available it gives an

283 indication of the potential improvements possible using stability information in a GPR model.

1. RESULTS

285 3.1 MIDAS site wind speed prediction

286 The GPR model was first used to show potential improvement on predicted 10 m wind speeds at 15 MIDAS locations. 9

287 months of data was used to train the model and learn the hyperparameters, and a further 3 months of data was used to test

288 the results.

289 Wind speeds predicted by the GPR model are compared to the MIDAS observations with several criteria used to assess

290 performance. Here three criteria are shown, mean absolute error (MAE), mean absolute percentage error (MAPE) and

291 root mean squared error (RMSE), calculated using equations (9), (10) and (11).

$$\text{MAE} = \frac{1}{n}\sum_{i=1}^{n}|y_t - \widehat{y}_t| \tag{9}$$

$$\text{MAPE} = \frac{1}{n}\sum_{i=1}^{n}\frac{|y_t - \widehat{y}_t|}{y_t} \times 100 \tag{10}$$

$$\text{RMSE} = \sqrt{\frac{1}{n}\sum_{i=1}^{n}(y_t - \widehat{y}_t)^2} \tag{11}$$

292 where y_t is the observed wind speed at time t, $\widehat{y}_t$ is the forecasted wind speed for the same time period and n is the

293 number of forecasts made. The comparison of different error metrics allows a full overview of the model performance.

294 The model errors are shown for a GPR model in which the datasets were split by stability class and a GPR model using

295 the full dataset. The results are shown alongside model errors for the wind speeds predicted by the simple GPR model

296 and the NWP prediction made by the Met Office. In order to fully illustrate the model results, detailed results are shown

297 for 4 of the 15 MIDAS sites tested, and summary results are shown for the 15 sites. In Figures 3 and 4 MAE and MAPE

298 are shown for 4 of the 15 MIDAS sites. This shows how the errors increase as the forecast period increases, and also how

299 the model error is reduced by using the GPR model with information on stability included. Overall, the simple GPR with

300 no information on stability reduces the error in predicted wind speed compared with predictions made by the NWP. The

301 improvement is site specific, with greatest error reduction seen at a forecast period 3 hours ahead for some sites, and

302 further ahead for others. Figure 5 shows a summary of errors over the 15 sites. This shows an average reduction in

MAPE of approximately 2% for the simple GPR model in comparison to wind speeds predicted by the NWP. For the GPR model with stability information, there is a reduction in MAPE of 5% for a 3 hour forecast period, rising to 9% for a 72 hour forecast period. The simple GPR model also shows an average of 2% improvement in MAE and RMSE for all forecast periods, whilst the GPR model with stability information shows a 10% improvement in MAE and a 7% improvement in RMSE.

In Figure 6 MAE and MAPE for the simple GPR model and the GPR with data subdivided by stability are shown in comparison to the persistence model. In addition to this, in Table 5, improvement over persistence is shown for MAE, RMSE and MAPE. It can be seen from this that there is a significant reduction in error in comparison to the persistence method for MAE, RMSE and MAPE. For the GPR model with stability, the reduction in MAPE over the persistence model is 14.5% at 3 hours ahead, increasing to 57.6% at 72 hours ahead.

In order to assess whether the errors seen for the GPR model are similar to other state of the art methods, some of the results seen in Table 1 are discussed. Figure 5 shows the average RMSE across the 15 sites for the GPR model with stability is 1.1 ms^{-1} at 3 hours ahead. At 1 hour ahead Li and Shi [35], Chen et al. [14] and Li et al.[36] give an RMSE of between 0.96 ms^{-1} and 1.5 ms^{-1}. Hence a RMSE of 1.1 ms^{-1} at 3 hours ahead is within the range of a good forecast. For the same three studies an MAE of between 0.72 ms^{-1} and 1.13 ms^{-1} is reported for a forecast 1 hour ahead. Figure 5 shows an average MAE of 0.82 ms^{-1} at 3 hours ahead for the GPR model with stability, again falling within the range shown by other studies.

At 72 hours the average RMSE for all 15 sites for the GPR model with stability is 1.54 ms^{-1} which is smaller than the RMSE reported by Louka et al. [16] of 2.38 – 2.88 ms^{-1} and Chen et al. [14] of 2.04 ms^{-1}. Similarly the average MAE over 15 sites for the same model at 72 hours ahead is 1.17 ms^{-1} compared to 1.75 – 2.04 ms^{-1} reported by Louka et al. [16] and 1.6 ms^{-1} reported by Chen et al. Furthermore the MAPE shown in Figure 5 for the GPR model with stability at 72 hours is 42%, slightly lower than the 44% reported by Chen et al. [14]. As different datasets are used to those in the literature discussed it is not possible to suggest that this model outperforms other model considered. However, the range of errors seen for the hybrid NWP and GPR model presented here are similar to those presented in literature, indicating some potential for this model for near surface wind speed prediction. In future, a comparison of other methods such as those summarised in Table 1 to the GPR model with atmospheric stability where the same dataset is used would be valuable.

Figure 3: MAE (with 95% confidence interval) for 4 sample MIDAS sites shown for GPR models both with and without stability, and the NWP.
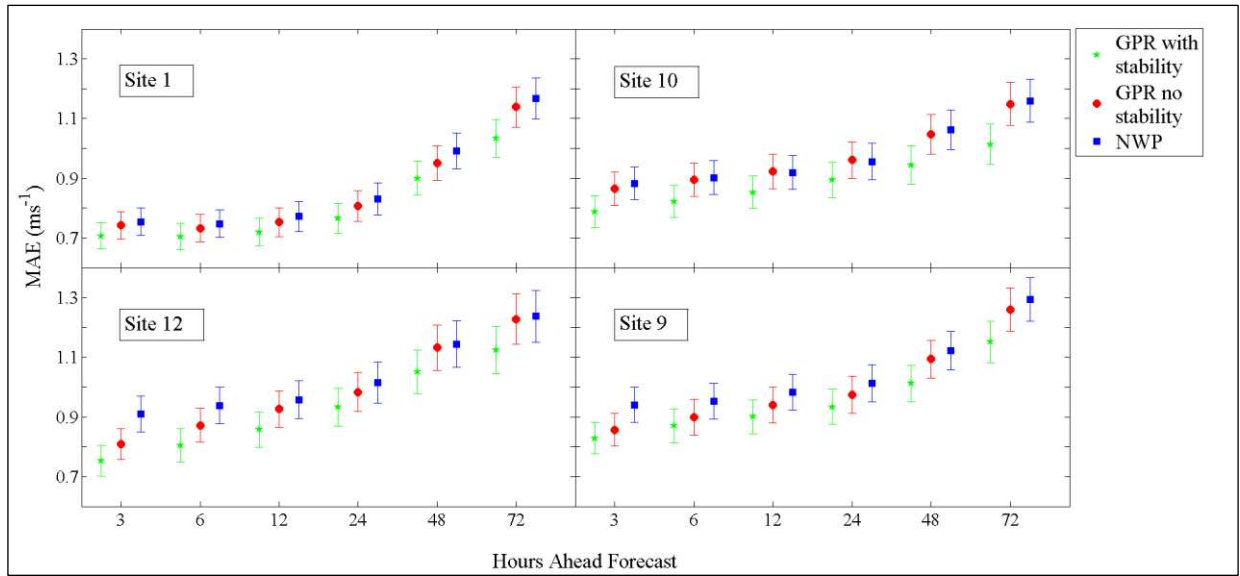
330

Figure 4: MAPE (with 95% confidence interval) for 4 sample MIDAS sites shown for GPR models both with and without stability, and the NWP.
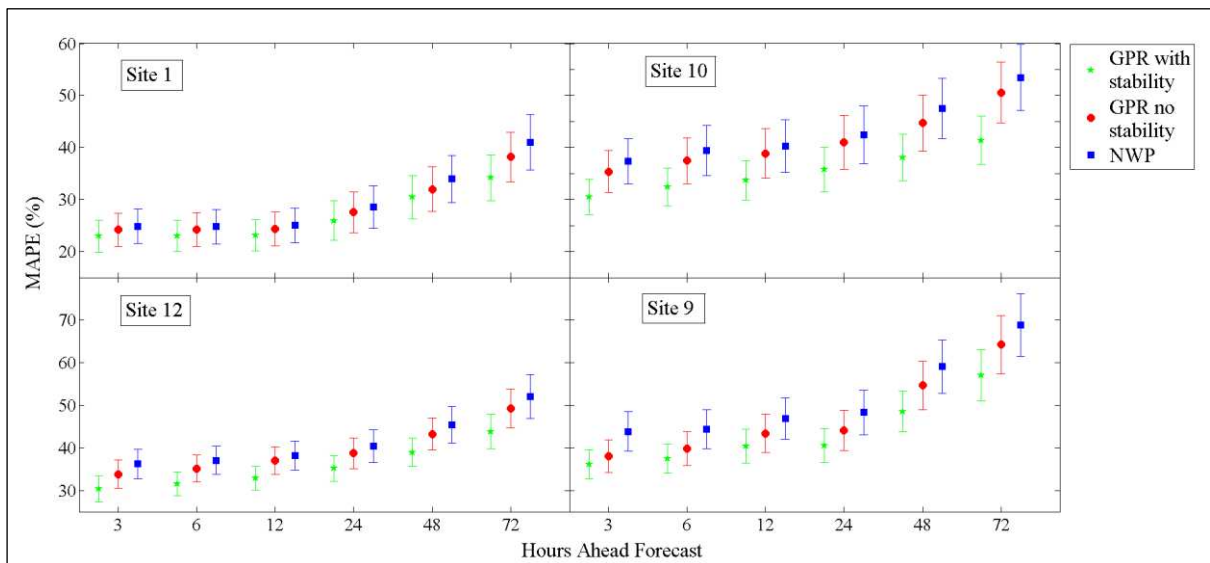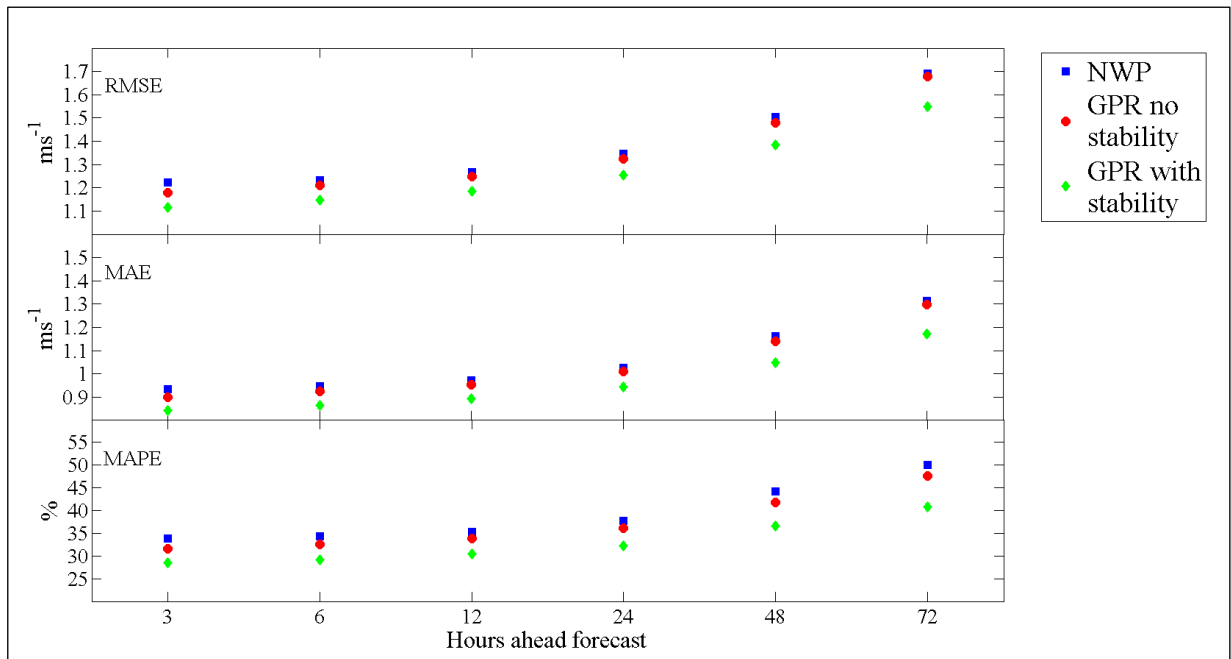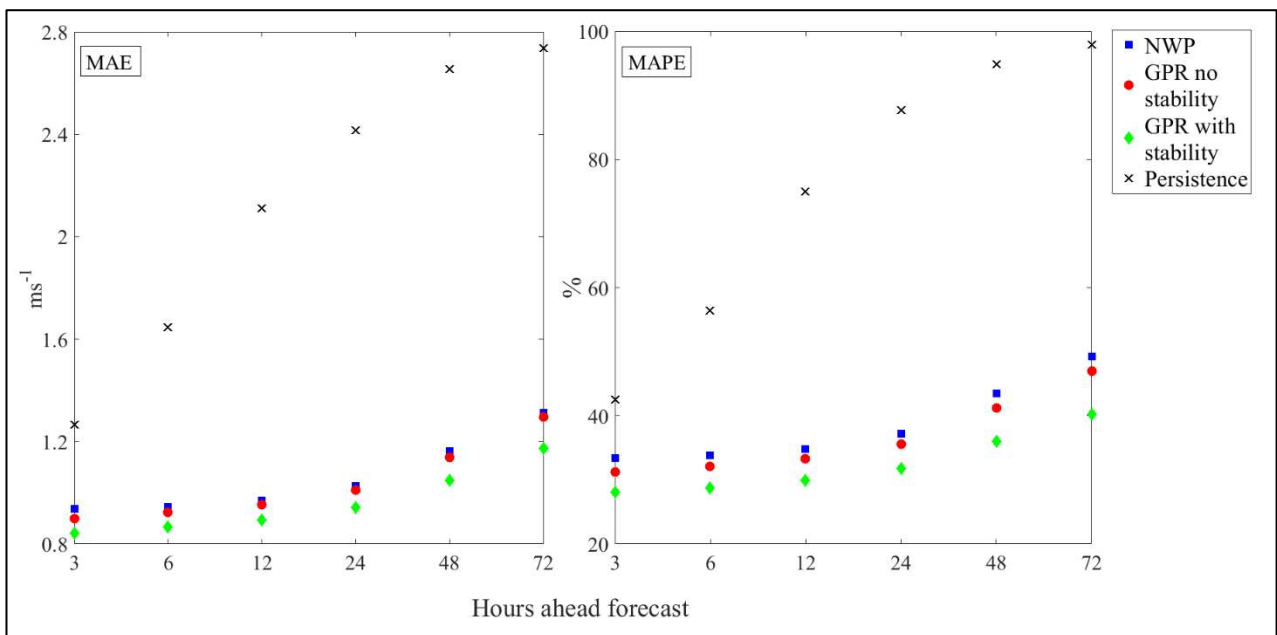

331

332

333

Figure 5: Average RMSE, MAE and MAPE for all 15 MIDAS sites. Error bars are not shown here to allow clarity.

334

Figure 6: Average MAE and MAPE for all 15 MIDAS sites shown in comparison to the persistence method.


335

336 Table 5: Improvement over the persistence method for both hybrid NWP and GPR models

Model	Error metric	Hours ahead forecast					
		3	6	12	24	48	72
GPR	MAE (ms^{-1})	0.38	0.73	1.16	1.42	1.52	1.45
	RMSE (ms^{-1})	0.43	0.83	1.29	1.45	1.25	0.63
	MAPE (%)	11.39	24.38	41.61	52.06	53.65	50.86
GPR with stability	MAE (ms^{-1})	0.43	0.79	1.22	1.48	1.65	1.57
	RMSE (ms^{-1})	0.58	0.98	1.45	1.65	1.54	1.07
	MAPE (%)	14.49	27.71	44.99	55.85	58.81	57.63

337

338 The model performance was also considered for the 4 different site categories observed; rural, urban, mountain and
339 coastal. Differing meteorological effects present different forecasting issues dependent on site characteristics. For
340 example at coastal sites wind speed is affected by changes in surface roughness, and availability of heat and moisture
341 [22]. In mountainous areas, complex orography and changes in temperature drive wind speed, and within urban areas
342 high densities of buildings can interfere with expected wind patterns. Taking this into account one might expect the
343 model results to vary with different site characteristics. Within the 15 MIDAS sites considered there was 1 mountain site,
344 3 coastal sites, 4 urban sites and 7 rural sites observed. Figure 7 shows how the Met Office NWP error varies within
345 different classifications. Average NWP error is shown for each site, calculated as an average over the time periods
346 considered (3 hours ahead, 6 hours ahead, up to 72 hours ahead). For the three coastal sites in the dataset, the average
347 model error is higher than for the rural and urban classifications. Only one mountain site is identified within the set,
348 hence it is difficult to suggest whether the results seen at this site are representative of all mountain sites however the
349 NWP error observed for this site is also higher than the rural and urban sites. The difference between errors in rural and
350 urban sites seems to be small, however, marginally higher errors are seen at the urban sites.

17

Figure 7: Average mean absolute error of the NWP forecast across all time periods considered (3 hours ahead – 72 hours ahead). A single average is shown for each site, with the sites split by site classification.
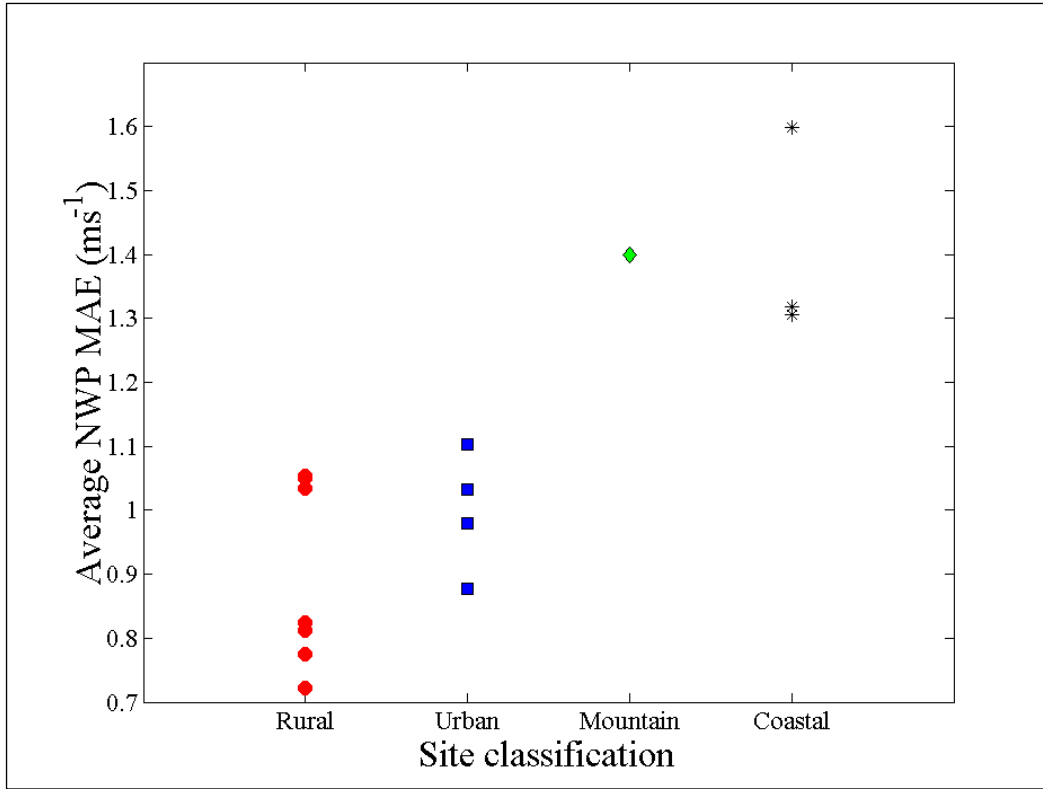

Having examined the NWP prediction error for different site classes, the reduction in error achieved using both GPR models is considered. This is calculated using equation 12.

$$\text{Reduction in average MAE} = \sum_{t=3}^{72} \left(MAE_{t,NWP} - MAE_{t,GPR} \right) \qquad (12)$$

where t is the time ahead forecasted. This reduction in error is shown in Figure 8 for both the simple GPR model and the GPR model with data subdivided by PGT stability class. It can be seen that for the simple GPR model lower errors are seen at all but one site. The site which did not achieve an improvement over the NWP was a rural site at which the NWP prediction error was the lowest of any sites considered, making it difficult to make enhanced predictions. Despite this, an improvement was seen when using GPR with stability at this site. Figure 8 shows that for the simple GPR the reduction in model error is not significantly different between site classes. However, for the GPR model subdivided by stability class a larger improvement is seen at coastal sites and at the mountain site. Given that in Figure 7 it was observed that coastal and mountain sites had the highest prediction errors from the NWP model this shows that the method improves upon sites where prediction accuracy is lower, which may be useful for wind farms located in regions with highly variable wind regimes. An improvement is also seen when using the GPR model with stability for prediction over both the simple GPR and the original NWP model in urban and rural areas, however, the achievement of the GPR model with stability is slightly less pronounced than for the coastal and mountain sites.

Figure 8: Reduction in error achieved by applying the GPR model compared to Met Office NWP model (A larger reduction indicates better model performance). (a) Shows results for simple GPR model, whilst (b) shows results for GPR model with data subdivided by PGT stability class.


(a)

(b)

365
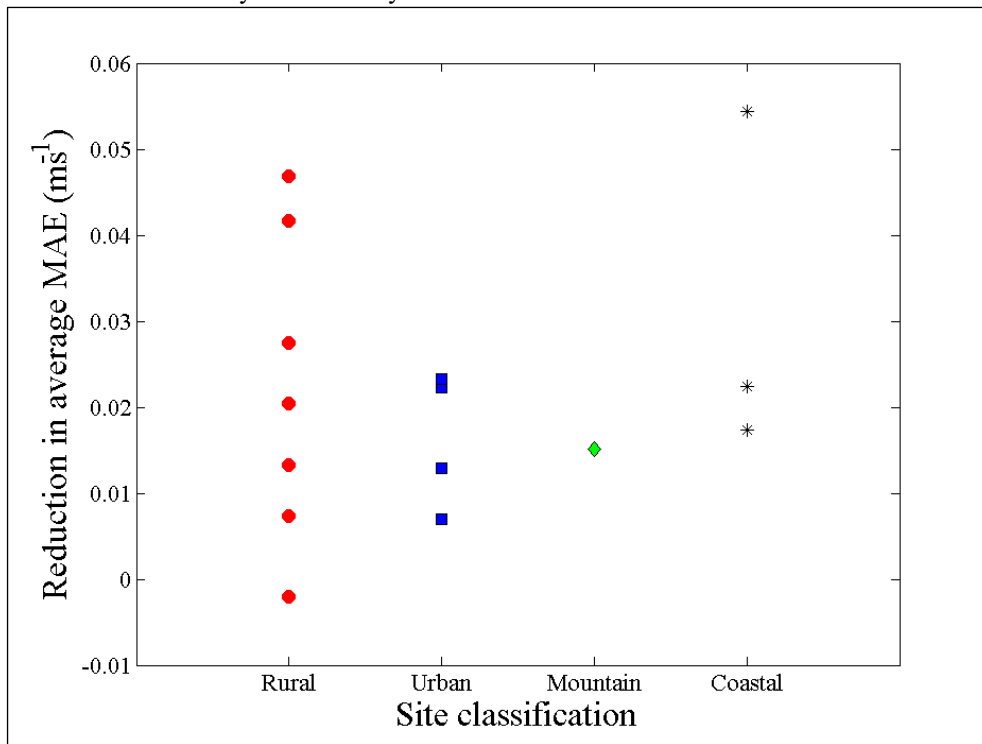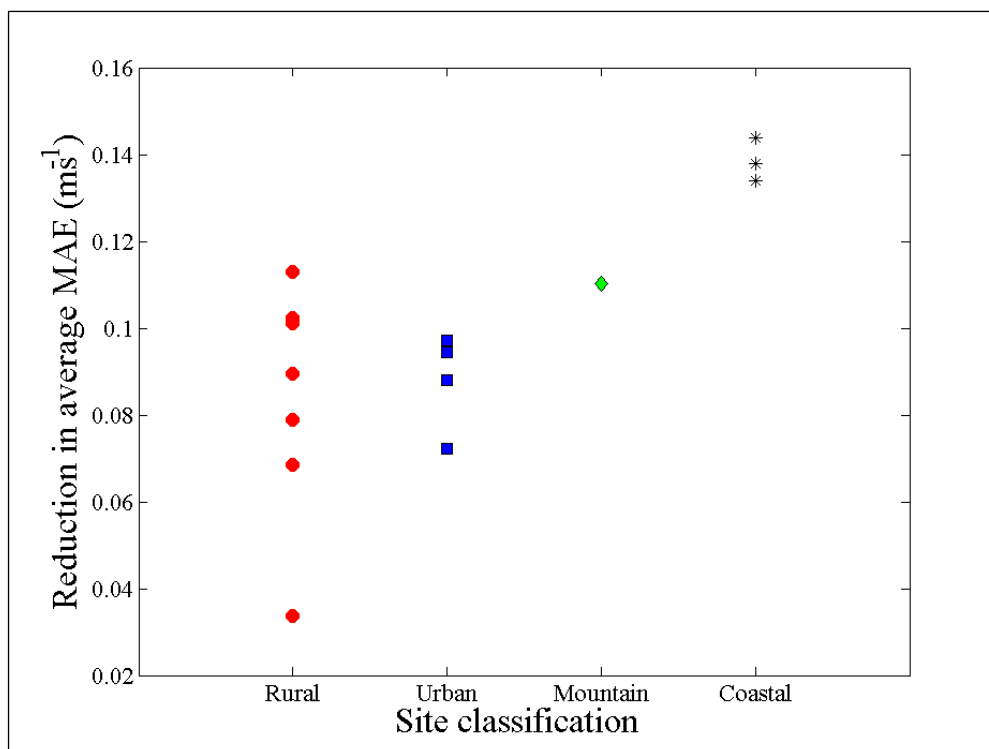
3.2 Hub Height Wind Speed Prediction

Whilst looking at predictions of 10 m wind speeds shows the potential of the GPR model and the importance of stability in reduction of model error, for wind power prediction hub height wind speed prediction is more important. Hub height wind speeds were obtained from the wind farm operator at one site in the UK for a 1.5 MW turbine. Power output and hub height wind speed data for wind turbines is generally difficult to obtain due to commercial sensitivity, hence only one dataset is used to show results for this work. Wind speed was measured at approximately 65 m above ground level. MIDAS data from an observation site located approximately 8 km from the turbine is used to calculate the stability class at the time of forecast, and the met office forecast data is taken from the same location as the MIDAS data. In Figure 9 MAPE and MAE are shown for hub height wind speed for both the simple GPR model and the GPR with data subdivided using PGT stability class. It shows a reduction on MAPE of between 1 and 2% and between 3 and 5% reduction in MAE using a GPR model with data subset by stability class. In Figure 9 the persistence results are omitted in order to show more clearly the difference between the two models, In Figure 10, the MAE, MAPE and RMSE for both GPR models are shown in comparison with a persistence model. It can be seen from Figure 10 that the GPR model shows significant improvements over the persistence model. In addition to this, in Table 6 the improvement in MAE, RMSE and MAPE over the persistence is displayed. This indicates that for the GPR model with stability there is a 7.5% reduction in MAPE at 3 hours ahead, rising to 31% at 72 hours ahead.

Taking the results for the GPR model with stability, a discussion of other methods seen in Table 1 allows the potential of this method to be considered. The GPR model with stability has an MAE of 0.95 ms^{-1} at 3 hours ahead, as shown in Figures 9 and 10. This is lower than some of the results shown in Table 1. For example, Chen et al. [14] report an MAE of between 0.72 and 1.1 ms^{-1} for a forecast between 1 and 4 hours ahead, Li and Shi [35] between 0.9 and 1.05 ms^{-1} for a forecast 1 hour ahead and Li et al. [36] 1.137 ms^{-1} at 1 hour ahead. Similarly the GPR model with stability has an RMSE of 1.2 ms^{-1} at 3 hours ahead, compared to Chen et al. [14] who reported between 0.96 and 1.95 for a forecast between 1 and 4 hours ahead, Li and Shi [35] who reported between 1.2 and 1.4 ms^{-1} for a forecast 1 hour ahead, and Li et al. [36] 1.5 ms^{-1} at 1 hour ahead. MAPE is only reported by Chen et al. [14] at between 11 and 17% for a forecast between 1 and 4 hours ahead. Figures 9 and 10 show MAPE from the current work as 17.5% at 3 hours ahead, which is slightly higher than Chen. However, the MAPE for the persistence model is also higher in the data shown in Figure 10 than for the results shown by Chen et al. At 72 hours ahead MAE for the GPR model with stability rises to 1.36 ms^{-1}. However, this is still lower than the results presented by Louka et al. and Chen et al. for this timescale in Table 1. Similarly, RMSE rises to 1.7 ms^{-1}, again lower than the results from Louka et al. and Chen et al. Figure 10 shows MAPE at 72 hours ahead for this model is 24%, which is 1% lower than for a GPR model without using stability, and 31% lower than the persistence method. MAPE is not given for predictions 72 hours ahead for any other model shown in Table 1. It is not possible to suggest overall superiority of one model whilst different datasets are used for different models presented in literature. However, considering the range of errors that a good forecast might achieve suggests that this model could provide good results for the prediction of hub height wind speed.

Figure 9: MAPE and MAE (with 95% confidence interval) for hub height wind speeds predicted with a simple GPR model and a GPR model with stability
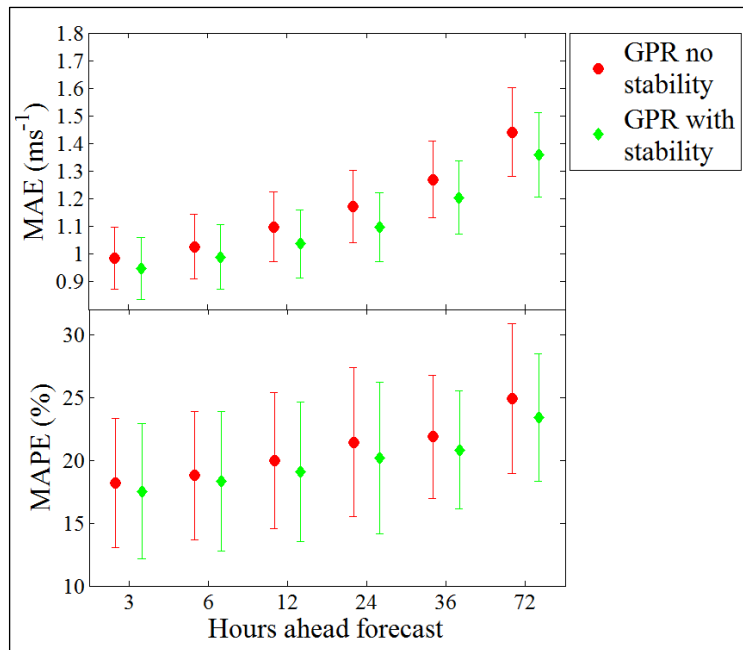
400

Figure 10: RMSE, MAE and MAPE for hub height wind speed predicted using GPR model with and without stability information. Persistence model is shown for comparison. Error bars are not shown here to allow clarity. Error bars for the GPR models can be seen in Figure 9.

401
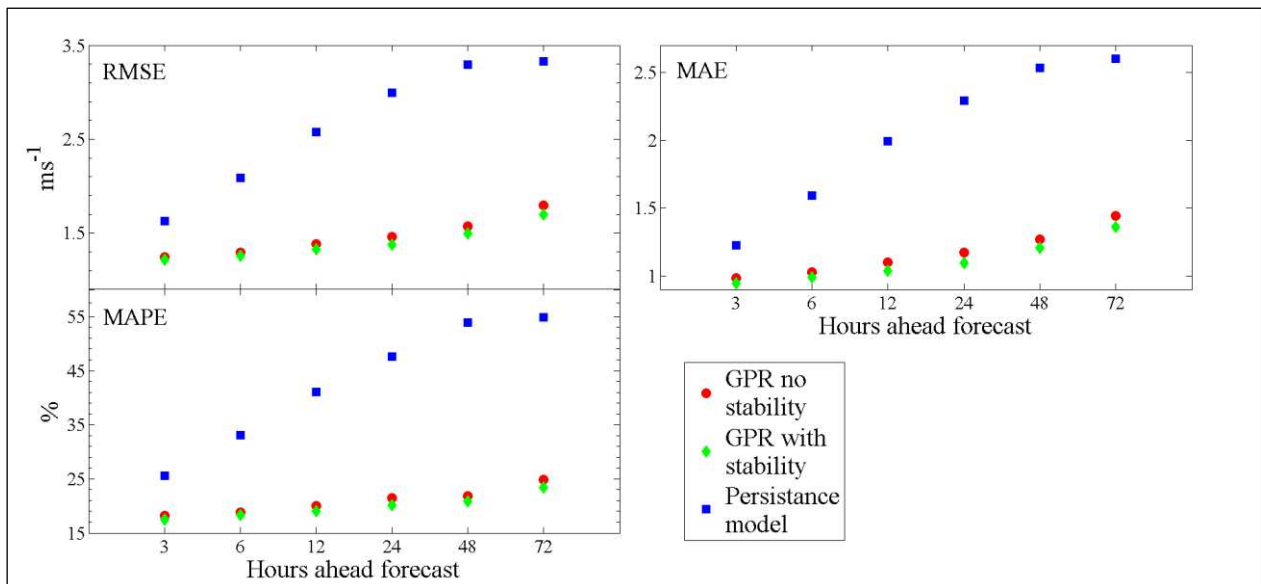
Table 6: Improvement in hub height wind speed predictions over persistence model.

Model	Error metric	Hours ahead forecast					
		3	6	12	24	48	72
GPR with stability	MAE (ms^{-1})	0.3	0.6	0.9	1.1	1.3	1.1
	RMSE (ms^{-1})	0.3	1.6	1.2	1.5	1.7	1.4
	MAPE (%)	7.5	14.7	21.9	27.6	32.2	31.1
GPR	MAE (ms^{-1})	0.3	0.6	1.0	1.2	1.3	1.3
	RMSE (ms^{-1})	0.4	1.7	1.3	1.6	1.8	1.6
	MAPE (%)	5.9	12.6	19.8	25.7	30.4	30.0

3.3 Significance of Results in Power Output Forecasting

In section 3.2, it can be seen that using a GPR to predict hub height wind speed leads to a reduction in prediction error in comparison to using the persistence method. Additionally, a further reduction is seen when the data is split using PGT stability class at the time of observation. In order to establish whether the reduction in error seen in hub height wind speed prediction is sufficient to suggest a reduction in power output prediction error, predicted power output is calculated from the predicted wind speed using a wind turbine power curve. A power curve is a relationship between wind speed and power output, which is specific to a turbine. They are usually provided by wind turbine manufacturers based on experimental data. Whilst they are not completely accurate for real data, they can give a crude estimate of predicted power output. In this case, the power curve is used to see whether the improved wind speed prediction offers any improvement in power output prediction. The turbine in use at the location in question is an old model, for which the manufacturer's power curve is not available. Hence the power curve used has been chosen from a database of available power curves and has been chosen such that the curve reflects the relationship between wind speed and power output data at the site as closely as possible.

In this section the model errors are shown as a percentage of turbine capacity, giving normalised MAE (NMAE) and normalised RMSE (NRMSE). This allows model results from larger or smaller turbines to be compared in a meaningful way. Hence the error metrics shown are given by equations 13 and 14.

$$NMAE = \frac{1}{n}\sum_{i=1}^{n}|y_t - \hat{y}_t| \times \frac{100}{C} \tag{13}$$

$$NRMSE = \sqrt{\frac{1}{n}\sum_{i=1}^{n}(y_t - \hat{y}_t)^2 \times \frac{100}{C}} \tag{14}$$

Where y_t is the observed wind speed at time t, $\hat{y}_t$ is the forecasted wind speed for the same time period, n is the number of forecasts made and C is the installed capacity of the turbine.

Figure 11 shows the difference in NMAE and NRMSE between power output predicted from wind speeds using a persistence model, a simple GPR model and a GPR model with stability classification. It shows a reduction in normalised MAE of between 2 and 12% for the power output predicted using wind speeds from the simple GPR model over a persistence model, and a further 0.5% for the GPR model split by stability class. Additionally, a reduction of between 4

427   and 16% in normalised RMSE for the simple GPR model compared to the persistence model with a further 0.5%

428   improvement using the GPR model with stability classes.

429   Due to the power curve for this turbine not being available the method for predicting power output could be improved

430   upon significantly however it shows that there may be some potential for improvement in power output forecast using the

431   GPR model with stability classes.

Figure 11: MAE and RMSE normalised by turbine capacity, shown for simple GPR and GPR with stability information

432
433
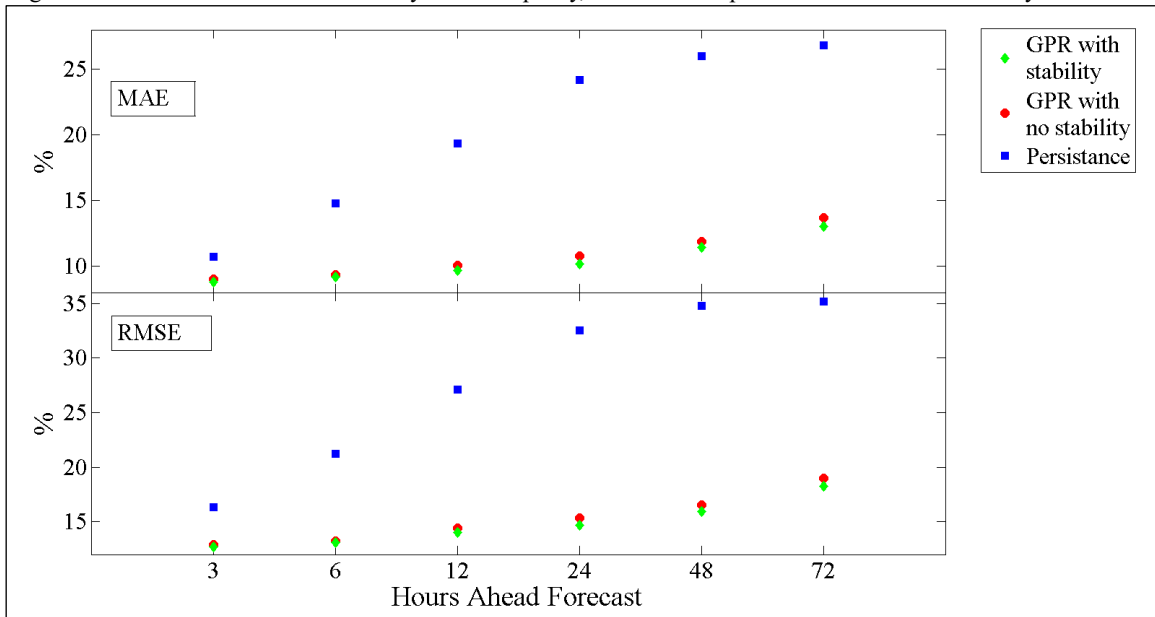
4. CONCLUSIONS AND FURTHER WORK

435   The motivation for this study has been to assess the performance of a hybrid numerical weather prediction model (NWP)

436   and Gaussian process regression (GPR) model in predicting near-surface wind speeds up to 72 hours ahead, and show

437   how subdividing data using the PGT atmospheric stability class can improve model performance. The results show that

438   when the simple GPR model is used for 10 m wind predictions there is a reduction in MAPE for all forecast periods of

439   2% over the NWP wind speed predictions. When the GPR model is used with data partitioned by atmospheric stability

440   there is a reduction in MAPE of 5% for forecasts made 3 hours ahead and 9% for forecasts made 72 hours ahead. This

441   indicates that the GPR model with data partitioned by stability class leads to improved wind speed predictions over the

442   NWP model. Particular improvements are seen at mountainous and coastal sites. Furthermore, using the GPR model

443   using data partitioned by stability class for the prediction of hub height wind speeds lead to a reduction in MAPE of

444   between 1 and 2% over the simple GPR model. It can also be seen that the improvements achieved using this model have

445   a positive impact on wind power output predictions. Implementing the GPR model with data partitioned by stability class

446   leads to a reduction in NMAE of 0.5% over the simple GPR model, and a reduction of between 2% and 12% in

447   comparison to the persistence methods. In general, the results seen for wind speed prediction are of comparable

448   magnitude to those observed in other methods listed in Table 1, as discussed in section 3.

449 The work so far demonstrates the potential of the method. With additional data improvements could be made to the

450 method shown. For example, due to the availability of forecasted weather variables, this work has so far relied upon the

451 use of stability class as calculated from observed weather variable rather than predicted stability class. Further work is

452 required to show a full predictive model with stability classes. To calculate the predicted stability conditions estimates of

453 other meteorological variables such as heat flux and frictional velocity are required, which are not routinely available. In

454 addition, the PGT stability class method is known to over-estimate the existence of neutral stability conditions. Other

455 methods could be used to calculate stability, potentially providing a more accurate representation of conditions. This may

456 increase the accuracy of this model further and provides an avenue for additional investigation in the future.

457 Whilst many methods for wind speed and power prediction exist, GPR has not been used widely for wind speed

458 prediction. Furthermore, despite the numerous methods that exist, the impact of atmospheric stability on predictions is

459 rarely considered. Because of this, the method provides a novel approach to forecasting and indicates promising results.

464 REFERENCES

465 [1] BEIS. *Renewable Energy Planning Database, extract December 2016*, Accessed: January 2017,
466 https://www.gov.uk/government/collections/renewable-energy-planning-data

467 [2] M.L. Ahlstrom, R.M. Zavadil. 2005, *The Role of Wind Forecasting in Grid Operations & Reliability*, IEEE/PES
468 Transmission & Distribution Conference & Exposition: Asia and Pacific, Dalian, China.

469 [3] R. Barthelmie, F. Murray, S. Pryor. 2008, *The economic benefit of short-term forecasting for wind energy in the UK*
470 *electricity market*, Energy Policy, 36, pp. 1687-1696.

471 [4] P. Coker, J. Barlow, T. Cockerill, D. Shipworth. 2013, *Measuring significant variability characteristics: An assessment*
472 *of three UK renewables*, Renewable Energy, 53, pp. 111-120.

473 [5] S.S. Soman, H. Zareipour, O. Malik, P. Mandal. 2010, *A review of wind power and wind speed forecasting methods*
474 *with different time horizons*, North American Power Symposium (NAPS).

475 [6] A. Costa, A. Crespo, J. Navarro, G. Lizcano, H. Madsen, E. Feitosa. 2008, *A review on the young history of the wind*
476 *power short-term prediction*, Renewable and Sustainable Energy Reviews, 12, pp. 1725-1744.

477 [7] J.L. Torres, A. García, M. De Blas, A. De Francisco. 2005, *Forecast of hourly average wind speed with ARMA models*
478 *in Navarre (Spain)*, Solar Energy, 79, pp. 65-77.

479 [8] R.G. Kavasseri, K. Seetharaman. 2009, *Day-ahead wind speed forecasting using f-ARIMA models*, Renewable Energy,
480 34, pp. 1388-1393.

481 [9] Met Office. *Met Office Numerical Weather Prediction models*, Accessed: June 2015 2015,
482 http://www.metoffice.gov.uk/research/modelling-systems/unified-model/weather-forecasting

483 [10] K.A. Larson, K. Westrick. 2006, *Short-term wind forecasting using off-site observations*, Wind Energy, 9, pp. 55-62.

484 [11] D. Wang, H. Luo, O. Grunder, Y. Lin. 2017, *Multi-step ahead wind speed forecasting using an improved wavelet*
485 *neural network combining variational mode decomposition and phase space reconstruction*, Renewable Energy, 113, pp.
486 1345-1358.

487 [12] C. Zhang, H. Wei, X. Zhao, T. Liu, K. Zhang. 2016, *A Gaussian process regression based hybrid approach for short-*
488 *term wind speed prediction*, Energy Conversion and Management, 126, pp. 1084-1092.

489 [13] J. Hu, J. Wang. 2015, *Short-term wind speed prediction using empirical wavelet transform and Gaussian process*
490 *regression*, Energy, 93, pp. 1456-1466.

491 [14] N. Chen, Z. Qian, X. Meng. 2013, *Multistep wind speed forecasting based on wavelet and gaussian processes*,
492 Mathematical Problems in Engineering, 2013, pp.

493 [15] E. Cadenas, W. Rivera, R. Campos-Amezcua, R. Cadenas. 2016, *Wind speed forecasting using the NARX model, case:*
494 *La Mata, Oaxaca, México*, Neural Computing and Applications, 27, pp. 2417-2428.

[16] P. Louka, G. Galanis, N. Siebert, G. Kariniotakis, P. Katsafados, I. Pytharoulis, G. Kallos. 2008, *Improvements in wind speed forecasts for wind power prediction purposes using Kalman filtering*, Journal of Wind Engineering and Industrial Aerodynamics, 96, pp. 2348-2362.

[17] J. Catalão, H. Pousinho, V. Mendes. 2011, *Short-term wind power forecasting in Portugal by neural networks and wavelet transform*, Renewable Energy, 36, pp. 1245-1251.

[18] I.J. Ramirez-Rosado, L.A. Fernandez-Jimenez, C. Monteiro, J. Sousa, R. Bessa. 2009, *Comparison of two new short-term wind-power forecasting systems*, Renewable Energy, 34, pp. 1848-1854.

[19] N. Chen, Z. Qian, I.T. Nabney, X. Meng. 2014, *Wind power forecasts using Gaussian processes and numerical weather prediction*, Power Systems, IEEE Transactions on, 29, pp. 656-665.

[20] F. Shu, J.R. Liao, R. Yokoyama, C. Luonan, L. Wei-Jen. 2009, *Forecasting the Wind Generation Using a Two-Stage Network Based on Meteorological Information*, Energy Conversion, IEEE Transactions on, 24, pp. 474-482.

[21] K. Ashrafi, G.A. Hoshyaripour. 2010, *A model to determine atmospheric stability and its correlation with CO concentration*, International Journal of Civil and Environmental Engineering, 2, pp.

[22] R.J. Barthelmie. 1999, *The effects of atmospheric stability on coastal wind climates*, Meteorological Applications, 6, pp. 39-47.

[23] C.E. Rasmussen, C.K.I. Williams. 2006, *Gaussian Processes for Machine Learning*, The MIT press, ISBN: 0-262-18253-X

[24] T. Chen, J. Morris, E. Martin. 2007, *Gaussian process regression for multivariate spectroscopic calibration*, Chemometrics and Intelligent Laboratory Systems, 87, pp. 59-71.

[25] D. Nguyen-Tuong, J.R. Peters, M. Seeger. 2009, *Local Gaussian process regression for real time online model learning*, Advances in Neural Information Processing Systems.

[26] H. He, W.C. Siu. 2011, *Single image super-resolution using Gaussian process regression*, IEEE Conference: Computer Vision and Pattern Recognition (CVPR).

[27] C.E. Rasmussen. 2006, *Gaussian processes for machine learning*, pp.

[28] D. Duvenaud. 2014, *Automatic model construction with Gaussian processes*, University of Cambridge, Doctoral Dissertation.

[29] Met Office. *3 hourly weather forecast and observational data - UK locations*, Accessed: September 2015, http://data.gov.uk

[30] Met Office. *Met Office Integrated Data Archive (MIDAS) Land and Marine Surface Stations Data (1853-current)*, Accessed: March 2015, http://catalogue.ceda.ac.uk/

[31] E.L. Petersen, N.G. Mortensen, L. Landberg, J. Højstrup, H.P. Frank. 1997, *Wind power meteorology*, Risø National Laboratory, Roskilde, Denmark, Technical Document No. Risø-I-1206 (EN), pp.

[32] J.S. Irwin. 1979, *A theoretical variation of the wind profile power-law exponent as a function of surface roughness and stability*, Atmospheric Environment (1967), 13, pp. 191-194.

[33] U. Focken, M. Lange, K. Mönnich, H.-P. Waldl, H.G. Beyer, A. Luig. 2002, *Short-term prediction of the aggregated power output of wind farms—a statistical analysis of the reduction of the prediction error by spatial smoothing effects*, Journal of Wind Engineering and Industrial Aerodynamics, 90, pp. 231-246.

[34] D.B. Turner. 1964, *A diffusion model for an urban area*, Journal of Applied Meteorology, 3, pp. 83-91.

[35] G. Li, J. Shi. 2010, *On comparing three artificial neural networks for wind speed forecasting*, Applied Energy, 87, pp. 2313-2320.

[36] G. Li, J. Shi, J. Zhou. 2011, *Bayesian adaptive combination of short-term wind speed forecasts from neural network models*, Renewable Energy, 36, pp. 352-359.